31st Annual International Conference of the IEEE EMBS
Minneapolis, Minnesota, USA, September 2-6, 2009

Transcranial Magnetic Stimulation of Small Animals: a Modeling Study of the Influence of Coil Geometry, Size and Orientation

R. Salvador and P. C. Miranda

Abstract— **Several recent studies have investigated the mechanisms of repetitive transcranial magnetic stimulation (rTMS) using small animals. However, there is still limited knowledge about the distribution of the induced electric field, and its dependence on coil size, geometry and orientation. In this work we calculate the electric field induced in a realistically shaped homogeneous mouse model by commercially available coils in several different orientations. The results show that the secondary field, resulting from charge accumulation at the skin – air interface, drastically changes the magnitude, decay and focality of the primary field induced by the coil. Accurate knowledge about the distribution of the field is invaluable in designing experimental protocols and new coils for small animal stimulation.**

I. Introduction

REPETITIVE transcranial magnetic stimulation (rTMS) is a recently developed tool which has been shown to have several potential basic neuroscience and clinical applications. However, the mechanisms that underlie the effects of rTMS remain largely unknown. This has lead to the appearance of several animal studies, the majority of which using rodents ([1]).

The results obtained with rTMS of small animals might not be, however, applicable to the human case. This is due to the fact that the coils typically used in rTMS are much larger than the head of small animals, which has been shown to highly reduce the electric field induced in the head during stimulation ([2]).

Another difficulty that hampers animal studies comes from the fact that there is still limited knowledge about the electric field distribution in rTMS. To overcome this, numerical studies have been used to calculate the electric field distribution in realistic rat models ([3]). These studies, however, use only a limited number of coil geometries and orientations.

In this work we use the finite element method to calculate the electric field induced in a realistically shaped homogeneous mouse model by coils with different geometries and orientations. The performance of each model is assessed by comparing the field's magnitude, decay with depth and focality. This work may prove useful in optimizing coil placement and orientation in order to stimulate a given target region of the rat's brain.

Manuscript received April 7, 2009. This work was supported by the Foundation for Science and Technology (FCT), Portugal. RS gratefully acknowledges the support of FCT under Grant SFRH/BD/23537/2005.

R. Salvador and P. C. Miranda are with the Institute of Biophysics and Biomedical Engineering, Faculty of Sciences, Lisbon 1749-016, Portugal (phone: +351217500177; fax: +351217500030; e-mail: rnsalvador@fc.ul.pt).

II. Methods

A. Mouse model

The model used in this study (see Fig. 1) was based on a previously built finite-element mesh of a mouse ([4]), available at: http://neuroimage.usc.edu/Digimouse.html. The surface mesh representing the skin was converted into an IGES file using Matlab (version 2008, www.mathworks.com) and 3Data Expert software (version 8.1, http://www.deskartes.com). The file was then read by the finite element program we used (Comsol 3.5, www.comsol.com) and converted into a solid. A similar procedure was employed to the outer surface of the brain which is also represented in the model. In order to reduce the finite element mesh complexity, only half of the mouse was meshed.

Despite the fact that the model includes the outer surface of the brain, the latter is not attributed different dielectric properties, and its only purpose is data visualization. The mouse is, therefore, modeled as a homogeneous and isotropic medium with an electrical conductivity of 0.33 S/m and a relative dielectric permittivity of 10^4, which have been shown to be valid for the low frequency values (< 10 kHz) of most TMS pulses ([5]).

B. Coil geometry and orientation

In this work we modeled two different circular coils and two different figure-8 coils, available from the Magstim Company. The details of these coils are summarized in Table I and further information can be found in [6] and [7].

The coils were oriented in different ways according to their geometry. Four different orientations were considered for the circular coils (see Fig. 2a-d) and two for the figure-8 coil (Fig. 2e-f).

C. Electric field calculation

The total electric field induced in the tissue by the coils was calculated using the finite element method, as implemented by Comsol. The latter allows for the calculation of the electric field under the quasi-static approximation, which is valid for the frequency range of most TMS pulses ([8]). The total electric field is the sum of two components ([9]): a non-conservative primary component that depends only on the geometry of the coil

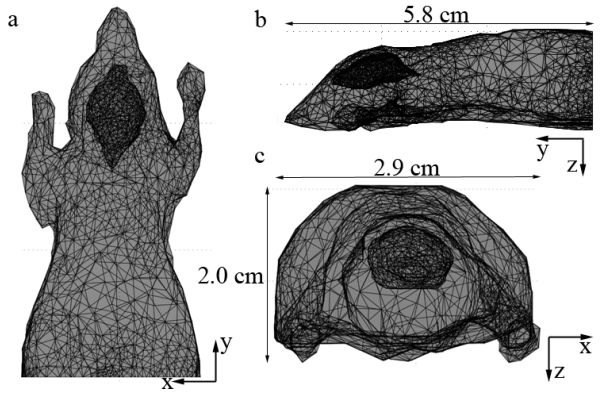

Fig. 1. Finite element mesh of the mouse model used in this work: (a) Top view of the model; (b) lateral view from the left; (c) frontal view. Also seen in the figure is the surface representing the mouse's brain. The y-axis points in the posterior-anterior (PA) direction, the x-axis in the right-left (RL) direction and the z axis in the dorsal-ventral direction.

and represents the field that would be induced in an infinite homogeneous medium, and a conservative secondary component that results from charge accumulation at boundaries that separate media with different electrical conductivities.

The values of the electric field displayed in the Results section were obtained at the time instant when the field is maximum. As the total electric field induced in TMS is proportional to the time derivative of the current in the coil ([8]), it is important to guarantee that we use realistic values for this parameter. For magnetic stimulators the maximum value of the current time derivative depends on the charging voltage of the capacitors (V_C) and on the inductance of the coil (L) according to the expression $di/dt\big|_{Max} = V_C / L$.

The values for the inductance of the coils modeled here are shown in Table I. In this study we modeled a stimulator based on the Magstim Rapid ([10]) model, because it is more suitable for rTMS applications. For this device the maximum stimulator output (MSO), i.e. 100 % on the front panel, corresponds to V_C=1650 V. However it can be programmed to go up to 120 % MSO (V_C=1980 V, [11]).

After adaptive meshing, the finite element mesh of the models comprised between 0.5 to 1.5 million tetrahedral first order elements, and took about 3 hours to solve on a computer with two dual core processors (Intel Xeon 5160) clocked at 3 GHz and 16 Gb of RAM memory.

D. Assessment of coil performance

For each coil orientation, we calculated the magnitude, decay and focality of the induced electric field. The magnitude and decay of the field were analyzed by considering lines that start at the maximum of the field at the brain's surface and end at a central point inside the brain. The focality was analyzed by determining the half power region (HPR, [12]) at the surface of the brain, which is defined as the area where the total electric field, $\vec{E}$, obeys the condition $\left\|\vec{E}\right\| \geq \left\|\vec{E}\right\|_{Max} \Big/ \sqrt{2}$. In order to obtain accurate results, we further refined the mesh along the lines and on the surface representing the brain.

TABLE I
PROPERTIES OF COILS USED IN THIS WORK

Coil	Geometry	Inductance (μH)
Circular 50 mm	Inner diameter: 25 mm Outer diameter: 77 mm Windings: 18	13.5[a]
Circular 70 mm	Inner diameter: 40 mm Outer diameter: 77 mm Windings: 15	16.25
Figure-8 25 mm	Inner diameter: 18 (×2) mm Outer diameter: 42 (×2) mm Windings: 14	10.11[a]
Figure-8 70 mm	Inner diameter: 56 (×2) mm Outer diameter: 87 (×2) mm Windings: 9	16.35

[a]These small coils need to be connected to a serial inductor when they are connected to the Magstim Rapid stimulator ([7]). The serial inductor increases the inductance of the coils by 4.89 μH.

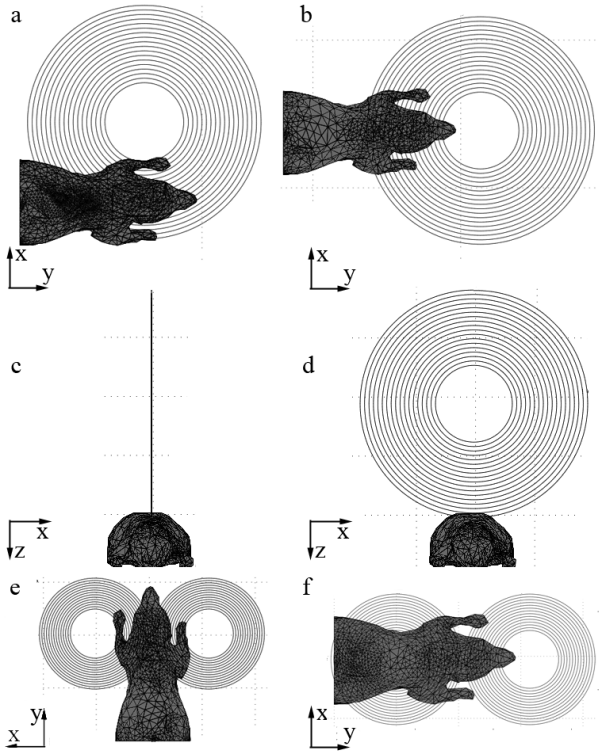

Fig. 2. Coil orientations modeled in the study. Models a, c, e / b, d, f will be referred to as PA / RL orientations, because that is the main direction of the field which they induce. (a) Circular coil shifted 50 mm (average diameter) to the left; (b) Same circular coil as in (a) but now shifted 50 mm towards the head's front; (c) and (d) Circular coil placed perpendicularly to the head; (e) Figure-8 coil (25 mm model) in the PA direction; (f) Figure-8 coil in the RL orientation. All the coils are placed approximately 2 mm above the head's surface.

III. RESULTS

A. Electric field distribution

The main direction of the primary component of the

electric field at the brain's surface is either PA (for the coil orientations depicted in Fig. 2a, c and e) or RL (Fig. 2b, d and f). The field along other directions is either very small (maximum of 25% of the value of the main component of the field for the circular coils) or completely negligible (figure-8 coils). The field's maximum, is always located at the region of the brain's surface closest to the coil (see Fig. 3a).

The secondary component of the electric field strongly reduces the main component of the primary field: at the brain's surface, the secondary field ranges from 67 % (PA oriented figure-8 25 mm coil, Fig. 2e) to 88 % (circular 70 mm coil oriented as in Fig. 2d) of the value of the primary field, along the main direction. The magnitude of the secondary field is greater for coil's oriented perpendicularly to the head and in the RL direction. The secondary field also affects the primary field along other directions, although less than it does along the main direction.

Due to the influence of the secondary component of the field, the total field has a much smaller magnitude than that of the primary component (see Fig. 3): the norm of the total field ranges from 12 % (circular 70 mm coil, oriented as in Fig. 2d) to 36 % (PA oriented figure-8 25 mm coil, Fig. 2e) of the primary field's norm. The field's distribution is also different; however the main direction of the field remains the same as for the primary component (see Fig. 3).

B. Field's magnitude and decay

The field due to charge accumulation not only reduces the magnitude of the field's primary component along the tested lines, but also increases its decay. This is illustrated in Fig. 4 for the case of the figure-8 25 mm coil. The two different coil orientations induce a similar primary component of the field, in terms of both magnitude and decay. However, the total electric field induced by the RL orientation has a smaller magnitude and decays more slowly than the field induced by the PA orientation (Fig. 4b).

In order to assess the capability of the different coil's used in this study to stimulate deeply located structures, we determined for each case the maximum depth (MD) at which the electric field remained larger than a reference value (RV) of 100 V/m, a value considered to be close to threshold for axon stimulation ([13]). At 75 % MSO, most coil orientations failed to induce a field larger than the RV along the test lines. The only exceptions were the circular coils oriented as shown in Fig. 2a (MD of 0.7 mm for the 50 mm coil and 0.4 mm for the 70 mm coil) and the figure-8 25 mm coil in both orientations (MD of 2.2 mm for the PA orientations and 1.3 mm for the RL orientation). Increasing the output to 120 % MSO increased the MDs for all the latter orientations to a maximum of 4 mm (figure-8 25 mm coil in both orientations). At this output, the circular coils oriented as shown in Fig 2b and the figure-8 70 mm coil with PA orientation also induced a field greater than the RV, with MDs of 0.6 mm, 0.1 mm and 1.9 mm, respectively.

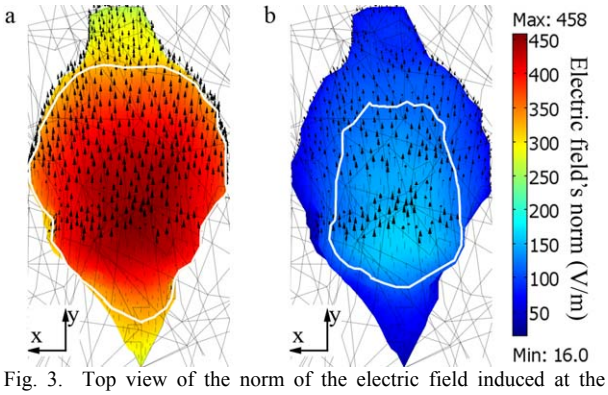

Fig. 3. Top view of the norm of the electric field induced at the brain's surface by a figure-8 25 mm coil with its central section oriented in the PA direction (y axis). (a) Primary component of the field; (b) Total electric field. The white lines encompass the HPR. These field values are for a stimulator output of 75 % MSO.

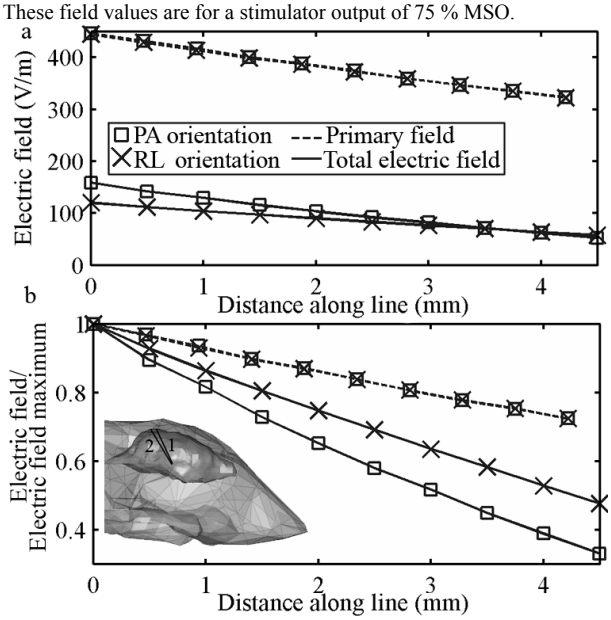

Fig. 4. Magnitude (a) and decay (b) of the electric field induced by a figure-8 25 mm coil along two test lines (see inset in b). Test line 1 is used to investigate the field's primary component, whereas test line 2 is used to investigate the total electric field. The two lines are different because the secondary field shifts the location of the field's maximum. The results in (a) were obtained for a stimulator's output of 75 % MSO.

With a smaller output of 50 % MSO, the only coil orientation that managed to induce a field larger than the RV was the figure-8 25 mm coil with PA orientation (MD of 0.3 mm).

C. Field's focality:

The focality of the primary component of the field is much worse than that of the total electric field. This is illustrated in Fig. 3 for the PA oriented figure-8 25 mm coil, although it applies to all other coil configurations. Globally, the HPR for the total electric field ranges from 15 % to 78 % of the value of the HPR for the primary field.

Another difference is that the HPR of the primary field depends essentially on the size of the coils, being largest for the figure-8 70 mm coil and smallest for the figure-8 25 mm coil. The HPR for the total field, however, depends more on the orientation of the coils than on their size. This is shown

by the fact that the HPR for the RL coil orientations is larger than that for PA orientations. Also, circular coils oriented perpendicularly tend to have better focality than those with a parallel orientation. Of all the coil orientations identified in the last section as being able to induce a field greater than the RV at 75 % MSO, the one with the best focality is the circular 50 mm coil, oriented as in Fig. 2a, with an HPR of 0.49 cm^2. For the figure-8 25 mm coil the HPR was 0.51 cm^2 and 1.1 cm^2 for the PA and RL orientations, respectively.

IV. Discussion

In this work we calculated the field induced in a model of a mouse's head by several different coils with various sizes and orientations. Consistent with what was found in an earlier work ([2]), many of the models studied here failed to induce a total electric field stronger than the RV in the mouse's brain, even at 120 % MSO. The decrease of the electric field with decreasing head's radius has been attributed to the fact that smaller heads capture a proportionately smaller fraction of the total flux of the magnetic field ([2]). This argument is based on the use of Faraday's law, which provides information only about the non-conservative primary component of the total electric field. In TMS, the contribution of the induced currents to the total magnetic field is negligible and so the distribution of the primary component of the electric field is determined solely by the geometry of the stimulation coil and is independent of the target size. The dependency on the target volume is introduced exclusively via charge accumulation at the boundaries, which generates the conservative secondary component. Thus, only the specification of the boundary shape can yield the total electric field in the general (quasistatic) case.

Our results show that the low total electric field results from this secondary field that tends to oppose the primary field, reducing it. For the same coil size, the secondary field increases with decreasing head's radius, which explains why the field induced in the mouse's head is low. The secondary field is also highly dependent on the geometry and orientation of the coils, which is seen by the different magnitude, decay and focality of the field induced by the different coils modeled in this study.

The smallest coils (circular 50 mm coil and figure-8 25 mm coil) proved to induce fields not only stronger than those induced by the biggest coils, but also with a smaller decay in depth. In terms of coil orientations, the only viable orientation for the circular coil was when it was placed parallel to the mouse's head inducing field in the PA direction (Fig. 2a). For the figure-8 coil, either the PA or RL orientations are capable of inducing a strong field that decays slowly.

Regarding the focality of the induced field, the results show that coil size has a smaller impact than coil orientation. For the most efficient coils, the circular 50 mm coil induces a more focal field than the figure-8 25 mm coil. Other coil orientations proved to have a better focality, mainly the perpendicular PA orientation for the circular coils. However these other orientations failed to induce a strong field at the brain surface rendering them ineffective in stimulating the mouse's brain.

The results presented here are for a homogeneous and isotropic model of a mouse. The main conclusions of this work should however hold for more realistic models, given that most charge accumulation in any model will always occur at the skin – air interface, which is correctly modeled in this work. In particular, the absence of the skull and CSF is not likely to have a significant effect on the results, given that the field induced in TMS does not have a significant radial component ([8]).

The present work highlights the importance of the field due to charge accumulation on the stimulation of mice with TMS. The results should hold qualitatively for other small animals such as rats or cats, but an accurate quantitative calculation of the field can only be obtained with numerical models. The latter are, therefore, important when designing experimental protocols and coils more suitable for small animal stimulation.

References

[1] S. H. Lisanby, and R. H. Belmaker, "Animal models of the mechanisms of action of repetitive transcranial magnetic stimulation (rTMS): Comparisons with electroconvulsive shock (ECS)," *Depression and Anxiety,* vol. 12, no. 3, pp. 178-187, 2000.

[2] J. D. Weissman, C. M. Epstein, and K. R. Davey, "Magnetic Brain-Stimulation and Brain Size - Relevance to Animal Studies," Electroencephalography and Clinical Neurophysiology, vol. 85, no. 3, pp. 215-219, Jun, 1992.

[3] J. Zheng, L. Li, and X. Huo, "Analysis of electric field in real rat head model during transcranial magnetic stimulation." pp. 1529-1532.

[4] B. Dogdas, D. Stout, A. F. Chatziioannou et al., "Digimouse: a 3D whole body mouse atlas from CT and cryosection data," Physics in Medicine and Biology, vol. 52, no. 3, pp. 577-587, Feb 7, 2007.

[5] S. Gabriel, R. W. Lau, and C. Gabriel, "The dielectric properties of biological tissues .2. Measurements in the frequency range 10 Hz to 20 GHz," Physics in Medicine and Biology, vol. 41, no. 11, pp. 2251-2269, Nov, 1996.

[6] R. Jalinous, Guide to magnetic stimulation, Magstim, Company, 1998.

[7] _____, Magstim® Coils & Accessories Operating Manual 1623-23-06, The Magstim Company 2005.

[8] B. J. Roth, L. G. Cohen, and M. Hallett, "The electric field induced during magnetic stimulation," Electroencephalogr Clin Neurophysiol Suppl, vol. 43, pp. 268-78, 1991.

[9] P. S. Tofts, and N. M. Branston, "The Measurement of Electric-Field, and the Influence of Surface-Charge, in Magnetic Stimulation," Electroencephalography and Clinical Neurophysiology, vol. 81, no. 3, pp. 238-239, Jun, 1991.

[10] _____, Magstim Rapid P/N 3576-23-08 Operating manual, The Magstim Company, 2006.

[11] T. Kammer, S. Beck, A. Thielscher et al., "Motor thresholds in humans: a transcranial magnetic stimulation study comparing different pulse waveforms, current directions and stimulator types," Clinical Neurophysiology, vol. 112, no. 2, pp. 250-258, Feb, 2001.

[12] R. Carbunaru, and D. M. Durand, "Toroidal coil models for transcutaneous magnetic stimulation of nerves," IEEE Transactions on Biomedical Engineering, vol. 48, no. 4, pp. 434-441, Apr, 2001.

[13] K. R. Davey, and M. Riehl, "Suppressing the surface field during transcranial magnetic stimulation," IEEE Transactions on Biomedical Engineering, vol. 53, no. 2, pp. 190-194, Feb, 2006.